ScientificScholar®
Knowledge is power
Publisher of Scientific Journals

www.clinicalimagingscience.org

Journal of Clinical Imaging Science

Original Research

Ultrasound Imaging Morphology is Associated with Biological Behavior in Invasive Ductal Carcinoma of the Breast

Gopal R. Vijayaraghavan[1], Matthew Kona[1], Abiramy Maheswaran[2], Dina H. Kandil[3], Madhavi K. Toke[2], Srinivasan Vedantham[4]

Departments of [1]Radiology, [2]Medical Oncology and [3]Pathology, University of Massachusetts Medical School, Worcester, Massachusetts, [4]Department of Medical Imaging, University of Arizona, Tucson, Arizona, United States.

***Corresponding author:**
Srinivasan Vedantham,
Department of Medical Imaging, University of Arizona, Tucson, Arizona, United States.

svedantham@arizona.edu

Received : 17 March 2021
Accepted : 11 August 2021
Published : 02 September 2021

DOI
10.25259/JCIS_60_2021

Quick Response Code:

ABSTRACT

Objectives: Ultrasound (US) is commonly used for diagnostic evaluation of breast lesions. The objective of this study was to investigate the association between US imaging morphology from routine radiologists' interpretation and biological behavior such as receptor status and tumor grade determined from histopathology in invasive ductal carcinoma (IDC).

Material and Methods: This retrospective study included 453 patients with pathology-verified diagnosis of IDC who had undergone US imaging and had surgery over a 5-year period. US and surgical pathology reports were reviewed and compiled. Correlation analyses and age-adjusted multivariable models were used to determine the association between US imaging morphology and receptor status, tumor grade, and germ line mutation of the breast cancer genes (BRCA1 and BRCA2). The odds ratio (OR), area under receiver operating characteristic curve (AUC), and 95% confidence intervals (CI) were obtained.

Results: The likelihood for high-grade cancer increased with size (OR: 1.066; CI: 1.042–1.091) and hypo-echogenicity (OR: 2.044; CI: 1.337–3.126), and decreased with angular or spiculated margins (OR: 0.605; CI: 0.393–0.931) and posterior acoustic shadowing (OR: 0.352; CI: 0.238–0.523). These features achieved an AUC of 0.799 (CI: 0.752–0.845) for predicting high-grade tumors. The likelihood for Estrogen Receptor-positive tumors increased with posterior acoustic shadowing (OR: 3.818; CI: 2.206–6.607), angulated or spiculated margins (OR: 2.596; CI: 1.159–5.815) and decreased with US measured tumor size (OR: 0.959; CI: 0.933–0.986) and hypoechoic features (OR: 0.399; CI: 0.198–0.801), and achieved an AUC of 0.787 (CI: 0.733–0.841). The likelihood for Progesterone Receptor-positive tumors increased with posterior acoustic shadowing (OR: 2.732; CI: 1.744–4.28) and angulated or spiculated margins (OR: 2.618; CI: 1.412–4.852), and decreased with US measured tumor size (OR: 0.961; CI: 0.937–0.985) and hypoechoic features (OR: 0.571; CI: 0.335–0.975), and achieved an AUC of 0.739 (CI: 0.689–0.790). The likelihood for Human epidermal growth factor receptor 2-positive tumors increased with heterogeneous echo texture (OR: 2.141; CI: 1.17–3.919) and decreased with angulated or spiculated margins (OR: 0.408; CI: 0.177–0.944), and was marginally associated with hypoechoic features (OR: 2.101; CI: 0.98–4.505) and circumscribed margins (OR: 4.225; CI: 0.919–19.4). The model with the aforementioned four US morphological features and achieved an AUC of 0.686 (CI: 0.614–0.758). The likelihood for triple-negative breast cancers increased with hypo-echogenicity (OR: 2.671; CI: 1.249–5.712) and decreased with posterior acoustic shadowing (OR: 0.287; CI: 0.161–0.513), and achieved an AUC of 0.739 (CI: 0.671–0.806). No statistical association was observed between US imaging morphology and BRCA mutation.

Conclusion: In this study of over 450 IDCs, significant statistical associations between tumor grade and receptor status with US imaging morphology were observed and could serve as a surrogate imaging marker for the biological behavior of the tumor.

Keywords: Invasive ductal carcinoma, Ultrasound, Tumor grade, Hormone receptor, Triple-negative breast cancer

INTRODUCTION

Ultrasound (US) imaging plays an important and established role in diagnosis of breast cancer, image guidance for biopsies, and as an adjunct to mammography for screening women with dense breasts. Tumor grade and receptor status have important implications for treatment, prognostication and prediction of nodal metastasis. Given the wide availability of the US imaging and the ease of performing US-guided biopsies,[1-5] establishing an association between US imaging morphology and grade and receptor status of the tumor could serve as a useful surrogate imaging marker.

Among breast cancer types, invasive ductal carcinoma (IDC) is the most common and accounts for 70–80% of all breast cancers.[6] Typically, IDC manifests as a mass on sonographic images and the presence of posterior acoustic shadowing is considered one of the important characteristics of malignancy. However, there is a growing body of evidence indicating that posterior acoustic shadowing is often associated with low-grade tumors[7-9] and hormone-receptor positive tumors.[8-10] Studies indicate that posterior acoustic enhancement is observed often in high-grade tumors[7-9] and in tumors with at least one negative hormone receptor.[8,9] In terms of acoustic texture, majority of malignancies manifest as hypoechoic lesions.[11] Although hyperechoic lesions are generally associated with benign lesions, it can occur in malignancies and is observed more often in lobular carcinoma compared to IDC.[12] In terms of shape, majority of malignancies appear with an irregular shape.[11] The association between tumor margin on US imaging and tumor grade is less clear. One study reported that high-grade IDCs are more likely to exhibit microlobulated margins,[11] whereas another study reported that circumscribed margins occur more often in high-grade tumors.[10] Studies have reported that circumscribed margin and an abrupt boundary are more likely in triple-negative tumors.[10,13] It has also been reported that some of the sonographic findings vary with age.[8] An attempt to identify US image features that were associated with germ line mutation of the breast cancer genes (BRCA1 and BRCA2) did not yield specific features.[14]

Motivated by the aforementioned studies, this investigation, probably the largest series to our knowledge, was conducted to determine if these observations could be verified, and if additional features can be identified after controlling for age, in a large cohort of IDCs. Hence, this study was aimed at identifying US image morphological features that are associated with: (1) receptor status, (2) histological grade, and (3) breast cancer genetic mutation (BRCA1 and BRCA2).

MATERIAL AND METHODS

Human subjects

This retrospective study was conducted at a North American academic center under an institutional review board-approved, Health Insurance Portability and Accountability Act-compliant protocol with waiver of informed consent. A query of the institutional cancer registry was conducted to identify all subjects diagnosed with breast cancer between the time period of January 2012 and December 2016. This query yielded a total of 1781 patients diagnosed with breast cancer. For this study, patients were included, if they satisfied all of the following inclusion criteria: had a pathological diagnosis of IDC, had US findings, had initial diagnosis established by US-guided biopsy, and had surgery (lumpectomy/mastectomy) at our institution. A total of 453 patients satisfied the inclusion/exclusion criteria and formed the analyzed cohort.

Data collection

For each subject in the analyzed cohort, the pathological reports and the US imaging reports were reviewed by a 4th-year radiology resident undergoing breast imaging rotation under the direct supervision of a breast imaging fellowship-trained, attending radiologist with more than 25 years of experience. During the time period used for data collection, all patients had undergone US imaging (IU-22, Philips Healthcare, Bothell, WA) using a 17–5 MHz or a 12–5 MHz linear array transducer. All US imaging interpretations were performed by breast imaging-fellowship trained radiologists with 2–15 years of experience after training. For the analysis determining the association between US imaging features and histopathology, the histopathology results from the surgical procedure were considered the reference standard or truth.

Data preparation

The maximum extent of the tumor measured along three orthogonal directions was used to determine the US measured size. The collected nominal, ordinal, and binary data were numerically coded. The ordinal scale for tumor differentiation was numerically coded as 3: poorly-differentiated or high-grade, 2: moderately-differentiated or medium-grade, and, 1: well-differentiated or low-grade.

Statistical methods

All continuous variables were tested for normal distribution (Shapiro–Wilk's test) and appropriate summary statistics were obtained. Correlations (Spearman rho) between US provided morphological features and histopathology were assessed. For binary histopathology outcome measures, multivariable logistic regression models were used to assess their association with US morphological features. US features that exhibited reasonable correlation with pathology ($P < 0.2$) were considered as potential predictors and stepwise selection were used to determine the final set of predictors

and to obtain the odds ratio (OR) along with the Wald's 95% confidence interval (CI). Receiver operating characteristic (ROC) analyses were performed and the area under the ROC curves (AUC) were obtained. Hosmer-Lemeshow goodness of fit test and leave-one out cross validation were performed. All multivariable logistic regression models employed Firth's bias correction.[15] Age was considered as a covariate due to the observation by Aho *et al*. that noted some of the US imaging characteristics varied with age.[8] For histopathology-provided ordinal outcome measure (tumor grade), ordered logistic regression was attempted. If the proportional odds assumption could not be satisfied, then a generalized linear model was fit by specifying a multinomial distribution and cumulative logit-link function. Effects associated with $P < 0.05$ were considered statistically significant. All analyses were performed using statistical software (SAS® version 9.4, SAS Institute Inc., Cary, NC).

Pathology criteria

We retrospectively reviewed the prior pathological reports from the electronic medical records [Table 1]. Both the biopsy and surgical specimen reports were reviewed to establish the final tumor type and grade. Formalin-fixed and paraffin embedded samples were used for tissue analysis. The cancer type, grade, and receptor status were evaluated. The cancer type was determined based on Eosinophilic and Hematoxylin staining and special stains, where applicable. The Scarff-Bloom Richardson System was used for grading. The invasive cancers were classified into well-differentiated (Grade 1), moderately-differentiated (Grade 2), and poorly-differentiated (Grade 3). For estrogen receptor (ER) and progesterone receptor (PR) status staining percentages >10% were considered positive. Human epidermal growth factor receptor 2 (HER2) testing was determined by immunofluorescence staining. The equivocal cases were further assessed by fluorescence *in situ* hybridization test to establish if the tumor was HER2 positive or not.

RESULTS

The age distribution satisfied the normality assumption ($P = 0.648$) and the mean ± SD was 60.9 ± 12.6 years. The US measured tumor size did not satisfy the normality assumption ($P < 0.001$). The median and inter-quartile range (IQR) was 14 mm and 9–19 mm, respectively. The results are organized by tumor grade, followed by receptor status and BRCA mutation. Table 2 summarizes the results from correlation analysis and from multivariable modeling.

Differentiation/Grade

Tumor differentiation graded on an ordinal scale (3: poorly-differentiated, 2: moderately-differentiated, and 1: well-differentiated) was positively correlated with US measured tumor size ($\rho = 0.365$, $P < 0.001$), circumscribed ($\rho = 0.115$, $P = 0.014$) or microlobulated ($\rho = 0.160$, $P < 0.001$) margins, heterogeneous echo texture ($\rho = 0.100$, $P = 0.033$), posterior enhancement ($\rho = 0.224$, $P = 0.009$) and hypoechoic lesions ($\rho = 0.201$, $P < 0.001$), and negatively correlated with angular or spiculated margins ($\rho = -0.138$, $P = 0.003$), isoechoic lesions ($\rho = -0.193$, $P < 0.001$), and posterior acoustic shadowing ($\rho = -0.235$, $P = 0.006$). The proportional odds assumption could not be satisfied ($P < 0.001$). Hence, a generalized linear model was fit. After adjusting for age, the likelihood for poorly differentiated tumor increased with US measured tumor size (OR: 1.066; CI: 1.042–1.091, $P < 0.001$), and hypoechoic features (OR: 2.044; CI: 1.337–3.126; $P = 0.001$), and decreased with angular or spiculated margins (OR: 0.605; CI: 0.393–0.931; $P = 0.022$), and posterior acoustic shadowing (OR: 0.352; CI: 0.238–0.523; $P < 0.001$). Figure 1 shows an example case of a high-grade, ER/PR positive tumor. [Figure 2] shows an example case of a low-grade, ER negative tumor. Follow-up multivariable logistic regression analysis was performed by dichotomizing to high-grade versus low- or moderate-grade tumors. The overall model was significant (likelihood ratio test, $P < 0.0001$) and satisfied Hosmer-Lemeshow goodness-of-fit test ($P = 0.807$). Figure 3 shows the ROC curve for the overall model with the aforementioned four US morphological features and achieved an AUC of 0.799 (CI: 0.752–0.845). Regarding US measured tumor size, the mean (IQR) for well differentiated, moderately differentiated, and poorly differentiated tumors were 10 (7–15) mm, 14 (9–20) mm, and 16.5 (12–25) mm, respectively.

Table 1: Histopathology of the analyzed cohort.

Invasive ductal cancers	***n*=453**
Differentiation	
Well differentiated	119/453 (26.3%)
Moderately differentiated	214/453 (47.2%)
Poorly differentiated	120/453 (26.5%)
Stage	
Stage I	261/453 (57.6%)
Stage II	143/453 (31.6%)
Stage III	32/453 (7.1%)
Stage IV	17/453 (3.8%)
Receptor status	
ER positive	369/453 (81.5%)
PR positive	322/453 (71.1%)
HER2 positive	55/453 (12.1%)
Triple-negative	63/453 (13.9%)
BRCA testing performed	134/453 (29.6%)
BRCA1 mutation	7/134 (5.2%)
BRCA2 mutation	8/134 (6.0%)

Table 2: Results from correlation analysis and multivariable modeling with surgical histopathology as the reference standard. The numerical coding scheme for histopathology is included. Italicized features indicate negative correlation or lower likelihood.

Histopathology	Correlation analysis	Multivariable modeling
with numerical coding	US imaging feature (Spearman ρ, *P*-value)	US imaging feature (Odds Ratio; Wald's 95% CI; *P*-value)
Differentiation	US measured tumor size (*P*=0.365, *P*<0.001)	US measured tumor size (OR: 1.066; CI: 1.042–1.091; *P*<0.001)
3: Poorly differentiated	Circumscribed margins (*P*=0.115, *P*=0.014)	Hypoechoic (OR: 2.044; CI: 1.337–3.126; *P*=0.001)
2: Moderately differentiated	Microlobulated margins (*P*=0.160, *P*<0.001)	Angular or spiculated margins (OR: 0.605; CI: 0.393–0.931; *P*=0.022)
1: Well differentiated	Heterogeneous echo texture (*P*=0.100, *P*=0.033) Posterior enhancement (*P*=0.224, *P*=0.009) Hypoechoic (*P*=0.201, *P*<0.001) Angular or spiculated margins (*P*=−0.138, *P*=0.003) Isoechoic (*P*=−0.193, *P*<0.001) Posterior acoustic shadowing (*P*=−0.235, *P*=0.006)	Posterior acoustic shadowing (OR: 0.352; CI: 0.238–0.523; *P*<0.001)
ER	Angulated or spiculated margins (*P*=0.158, *P*<0.001)	Angulated or spiculated margins (OR: 2.596; CI: 1.159–5.815; *P*=0.017)
1: ER positive	Non-parallel orientation (*P*=0.101, *P*=0.032)	Posterior acoustic shadowing (OR: 3.818; CI: 2.206–6.607; *P*<0.001)
0: ER negative	Isoechoic (*P*=0.103, *P*=0.028) Posterior acoustic shadowing (*P*=0.284, *P*<0.001) US measured tumor size (*P*=−0.182, *P*<0.001) Microlobulated margins (*P*=−0.130, *P*=0.006) hypoechoic (*P*=−0.110, *P*=0.019) Posterior enhancement (*P*=−0.210, *P*<0.001)	US measured tumor size (OR: 0.959; CI: 0.933–0.986; *P*<0.001) Hypoechoic (OR: 0.399; CI: 0.198–0.801; *P*=0.001).
PR	Angulated or spiculated margins (*P*=0.158, *P*<0.001)	Angulated or spiculated margins (OR: 2.618; CI: 1.412–4.852; *P*=0.002)
1: PR positive	Non-parallel orientation (*P*=0.101, *P*=0.032)	Posterior acoustic shadowing (OR: 2.732; CI: 1.744–4.28; *P*<0.001)
0: PR negative	Isoechoic (*P*=0.103, *P*=0.028) Posterior acoustic shadowing (*P*=0.284, *P*<0.001) US measured tumor size (*P*=−0.182, *P*<0.001) Microlobulated margins (*P*=−0.130, *P*=0.006) Hypoechoic (*P*=−0.110, *P*=0.019)	US measured tumor size (OR: 0.961; CI: 0.937–0.985; *P*=0.001) Hypoechoic (OR: 0.571; CI: 0.335–0.975; *P*=0.04)

(Contd...)

Table 2: *(Continued)*

Histopathology	Correlation analysis	Multivariable modeling
	Posterior enhancement (*P*=−0.210, *P*<0.001)	
HER2 1: HER2 positive 0: HER2 negative	US measured tumor size (*P*=0.143, *P*=0.002) Circumscribed margins (*P*=0.104, *P*=0.027) Heterogeneous echo texture (*P*=0.122, *P*=0.009) Angulated or spiculated margins (*P*=−0.095, *P*=0.043) Posterior acoustic shadowing (*P*=−0.097, *P*=0.039)	Heterogeneous echo texture (OR: 2.141; CI: 1.17–3.919; *P*=0.014) Angulated or spiculated margins (OR: 0.408; CI: 0.177–0.944; *P*=0.036)
TNBC 1: TNBC 0: Not TNBC	US measured tumor size (*P*=0.123, *P*=0.009) Hypoechoic (*P*=0.113, *P*=0.016) Posterior enhancement (*P*=0.156, *P*=0.001) Age (*P*=−0.147, *P*<0.002) Angular or spiculated margins (*P*=−0.118, *P*=0.012) Isoechoic tumors (*P*=−0.096, *P*=0.042) Posterior acoustic shadowing (*P*=−0.219, *P*<0.001)	Hypoechoic (OR: 2.671; CI: 1.249–5.712; *P*=0.011) Posterior acoustic shadowing (OR: 0.287; CI: 0.161–0.513; *P*<0.001)

US: Ultrasound, OR: Odds ratio, CI: Confidence interval, ER: Estrogen receptor, PR: Progesterone receptor, HER2: Human epidermal growth factor, TNBC: Triple negative breast cancers

Receptor status

Estrogen-receptor (ER) positive cancers were significantly correlated with angulated or spiculated margins ($\rho = 0.158$, $P < 0.001$), non-parallel orientation ($\rho = 0.101$, $P = 0.032$), isoechoic tumors ($\rho = 0.103$, $P = 0.028$), and posterior acoustic shadowing ($\rho = 0.284$, $P < 0.001$), and were negatively correlated with US measured tumor size ($\rho = -0.182$, $P < 0.001$), microlobulated margins ($\rho = -0.130$, $P = 0.006$), hypoechoic tumors ($\rho = -0.110$, $P = 0.019$) and posterior enhancement ($\rho = -0.210$, $P < 0.001$). Age-adjusted multivariable logistic regression model indicated that the likelihood for ER-positive tumors increased with posterior acoustic shadowing (OR: 3.818; CI: 2.206–6.607; $P < 0.001$), angulated or spiculated margins (OR: 2.596; CI: 1.159–5.815; $P = 0.017$) and decreased with US measured tumor size (OR: 0.959; CI: 0.933–0.986; $P < 0.001$) and hypoechoic features (OR: 0.399; CI: 0.198–0.801; $P = 0.001$). Figure 4a shows the ROC curve with the aforementioned four US morphological features as predictors of ER-positive tumors and achieved an AUC of 0.787 (CI: 0.733–0.841).

Since PR positive cancers were significantly correlated with ER status ($P = 0.748$, $P < 0.001$), the same set of US morphological features as ER status were also significantly correlated ($P < 0.028$) with PR status. Age-adjusted multivariable logistic regression model indicated that the likelihood for PR-positive tumors increased with posterior acoustic shadowing (OR: 2.732; CI: 1.744–4.28; $P < 0.001$) and angulated or spiculated margins (OR: 2.618; CI: 1.412–4.852; $P = 0.002$), and decreased with ultrasound measured tumor size (OR: 0.961; CI: 0.937–0.985; $P = 0.001$) and hypoechoic features (OR: 0.571; CI: 0.335–0.975; $P = 0.04$). Figure 4b shows the ROC curve for differentiating PR-positive from PR-negative tumors with the aforementioned four US morphological features and achieved an AUC of 0.739 (CI: 0.689–0.790).

Human epidermal growth factor receptor 2 (HER2) positive cancers were significantly correlated with US measured tumor size ($\rho = 0.143$, $P = 0.002$), circumscribed margins ($\rho = 0.104$, $P = 0.027$), and heterogeneous echo texture

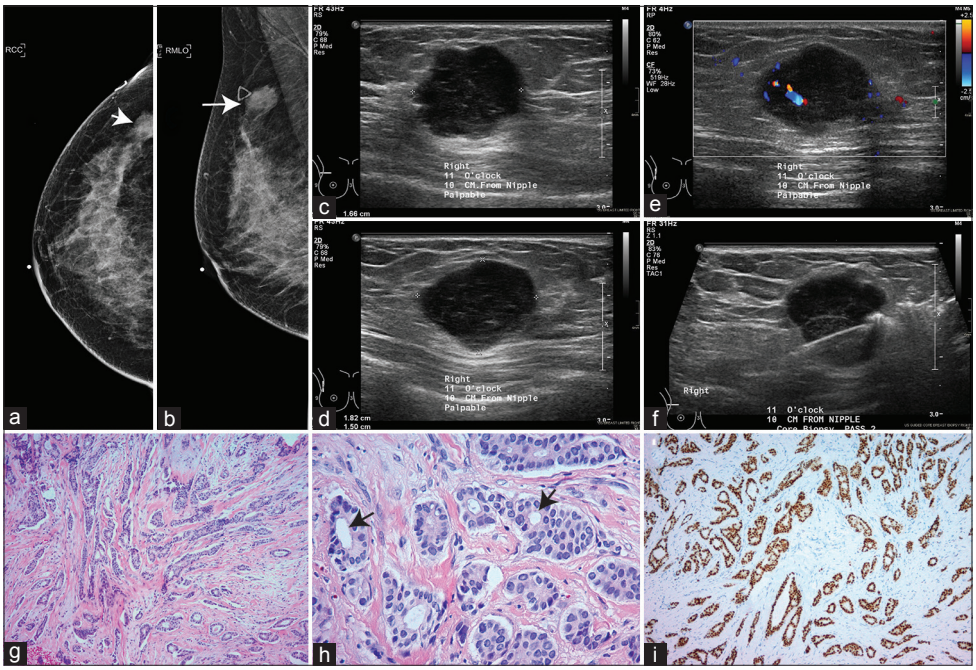

Figure 1: A 37-year-old woman with a palpable mass on the upper outer quadrant of the right breast. (a) Cranio-caudal mammogram. (b) Mediolateral Oblique mammogram. Arrows in (a and b) mark the lesion. The triangular skin marker indicating the location of the palpable mass is visible in (b). (c-e) Ultrasound imaging show a circumscribed 1.6 × 1.8 × 1.5 cm hypoechoic mass with flow and post enhancement at 11 o'clock position and 10 cm from nipple corresponding to the mass in mammograms. (f) Ultrasound image from biopsy procedure showing the needle. (g) invasive ductal carcinoma, grade 1, showing infiltrating malignant glands within desmoplastic stroma (H&E stain). (h) high-power magnification showing predominant tubular formation (arrows), mild nuclear atypia with rare/no mitosis (H&E stain). (i) ER immunostain showing strong diffuse positivity with anti-ER antibody.

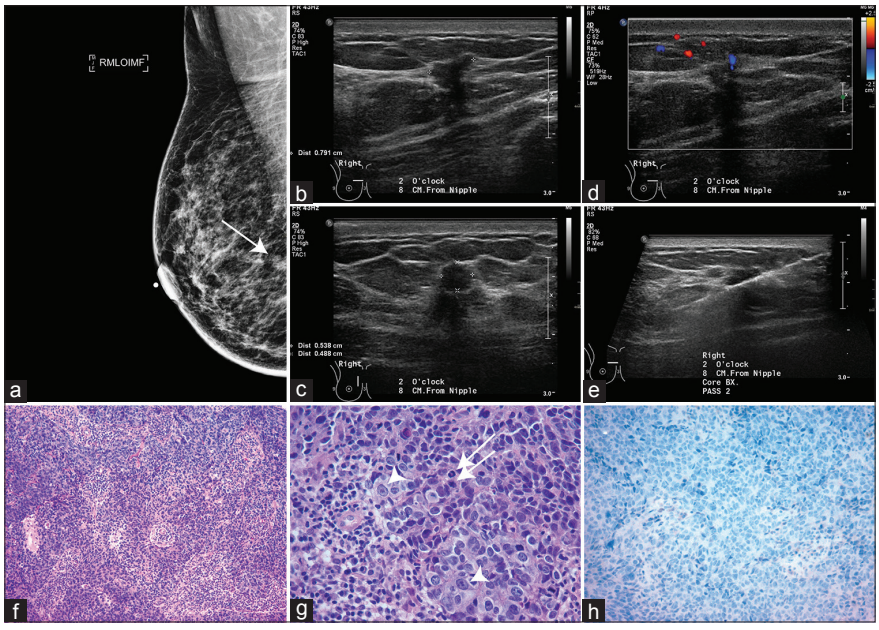

Figure 2: A 54-year-old woman with spiculated mass on a screening mammogram in the upper inner quadrant of the right breast. (a) Mediolateral oblique view. (b-d) show an irregular, hypoechoic mass measuring 5 x 5 x 8 mm with angular margins and posterior acoustic shadowing at 2 o'clock position and at 8 cm from the nipple corresponding to the spiculated mass on mammography. (e) Ultrasound image from biopsy procedure showing the needle. (f) invasive ductal carcinoma, grade 1, showing malignant cells in sheets with tumor infiltrating lymphocytes (H & E stain). (g) High-power view showing numerous mitosis (arrows) and marked nuclear pleomorphism (arrowheads). (h) Estrogen receptor immunostain shows negative staining.

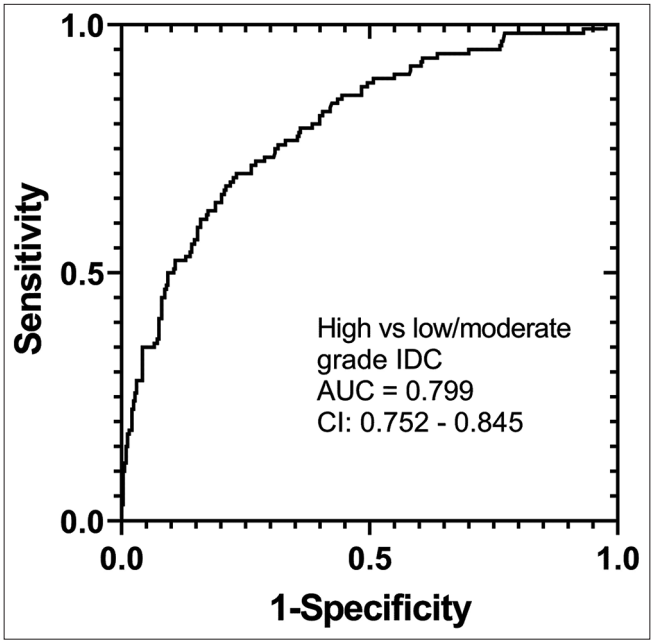

Figure 3: The receiver operating characteristic from multivariable logistic regression model for differentiating high versus low or moderate grade invasive ductal carcinoma with ultrasound morphological features of size, hypo-echogenicity, angular or spiculated margins, and posterior acoustic shadowing as predictors.

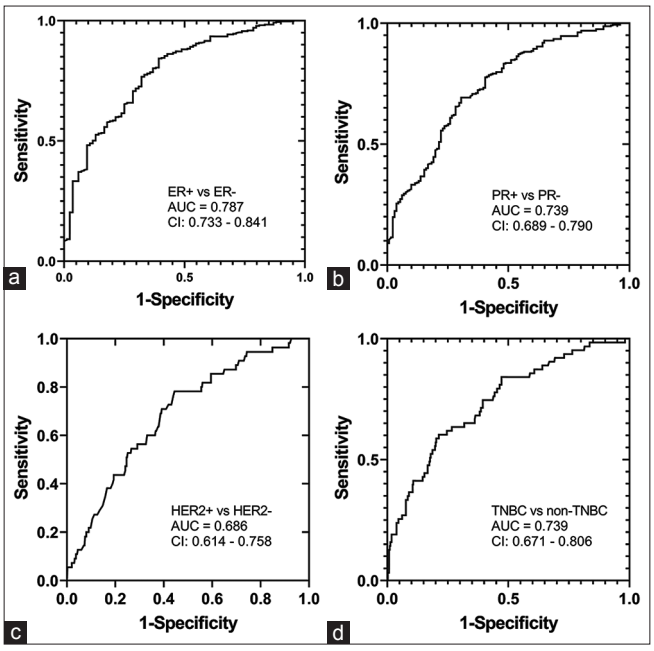

Figure 4: Receiver operating characteristic curves from age-adjusted multivariable logistic regression models with ultrasound morphological features as predictors to differentiate (a) ER-positive from ER-negative, (b) PR-positive from PR-negative, (c) HER2-positive from HER2-negative, and (d) TNBC from non-TNBCs. ER: Estrogen receptor, PR: Progesterone receptor, HER2: Human epidermal growth factor receptor 2, TNBC: Triple negative breast cancers.

(ρ = 0.122, P = 0.009), and were negatively correlated with angulated or spiculated margins (ρ = −0.095, P = 0.043) and posterior acoustic shadowing (ρ = −0.097, P = 0.039). HER2 status was marginally correlated with hypoechoic tumors (ρ = 0.087, P = 0.065). Age-adjusted multivariable logistic regression model indicated that the likelihood for HER2-positive tumors increased with heterogeneous echo texture (OR: 2.141; CI: 1.17–3.919, P = 0.014) and decreased with angulated or spiculated margins (OR: 0.408; CI: 0.177–0.944; P = 0.036). In addition, the likelihood for HER2 positive tumors showed a statistically marginal association with hypoechoic features (OR: 2.101; CI: 0.98–4.505; P = 0.056) and circumscribed margins (OR: 4.225; CI: 0.919–19.4; P = 0.064). Figure 4c shows the ROC curve for the differentiating HER2-positive from HER2-negative tumors with the aforementioned four US morphological features and achieved an AUC of 0.686 (CI: 0.614–0.758).

Triple negative breast cancers (TNBCs) constituted 63/453 (13.9%) of the analyzed cohort. TNBCs were positively correlated with US measured tumor size (ρ = 0.123, P = 0.009), hypoechoic lesions (ρ = 0.113, P = 0.016), and posterior enhancement (ρ = 0.156, P = 0.001), and were negatively correlated with age (P = −0.147, P < 0.002), angular or spiculated margins (ρ = −0.118, P = 0.012), isoechoic tumors (ρ = −0.096, P = 0.042), and posterior acoustic shadowing (ρ = −0.219, P < 0.001). Age-adjusted multivariable logistic regression model indicated that the likelihood for triple-negative breast cancers increased with hypoechoic features (OR: 2.671; CI: 1.249–5.712; P = 0.011) and decreased with posterior acoustic shadowing (OR: 0.287; CI: 0.161–0.513, P < 0.001). The model with the above mentioned US morphological features achieved an AUC of 0.739 (CI: 0.671–0.806) for identifying triple-negative breast cancers [Figure 4d].

All multivariable logistic regression models were significant (likelihood ratio test, P < 0.0014) and satisfied the Hosmer-Lemeshow goodness-of-fit tests (P > 0.374).

BRCA mutation

Among 453 subjects, 134/453 (29.6%) had BRCA testing. Only 7/134 (5.2%) were BRCA1 positive and 8/134 (6%) were BRCA2 positive. Although BRCA1 status was positively correlated with posterior enhancement (P = 0.224, P = 0.009) and was negatively correlated with posterior acoustic shadowing (P = −0.235, P = 0.006), age-adjusted multivariable logistic regression model did not identify these features to be predictive of BRCA1 mutation. None of the US features were correlated with BRCA2 mutation.

DISCUSSION

In a retrospective study of 120 IDCs, it was reported that posterior acoustic shadowing was observed often in low-

grade tumors than in high-grade tumors (71% vs. 28%), and posterior acoustic enhancement (36%) and well-defined margin (16%) were present in a substantial proportion of high-grade tumors.[7] A similar observation of posterior acoustic shadowing was more likely to occur in low-grade tumors was made by Aho *et al*.[8] Irshad *et al*.[9] observed increased likelihood of low-grade tumors when posterior shadowing is present and increased likelihood of high-grade tumors when posterior enhancement is present. In a study of 299 IDCs by Blaichman *et al*., high-grade tumors were associated with posterior enhancement, abrupt interfaces and microlobulated margins.[11] Celebi *et al*. studied 201 invasive breast cancers and noted that lesions with posterior acoustic shadowing were more likely to be of low histologic grade.[10] Our results are broadly consistent with the prior literature in that we observed a statistical relationship between lack of posterior acoustic shadowing, but not necessarily posterior enhancement, as a significant feature of poorly-differentiated, high-grade tumors. We identified additional US features pertaining to echogenicity and margins that were associated with high-grade tumors. Specifically, after adjusting for age and size (i.e., when age and size are maintained constant), tumors with hypoechoic features have >2 times the odds for poorly differentiated tumor. Furthermore, tumors that lack angular or spiculated margins have lower (0.6 times) odds for being high-grade. Echoic features were classified as hyper, iso or hypo-echoic according to BI-RADS criteria and no additional grading was performed.

Regarding receptor status, Aho *et al*.[8] also noted that posterior acoustic enhancement was more common in ER negative tumors and that some of the sonographic characteristics varied with age. Irshad *et al*. also observed increased likelihood of ER positive tumors when posterior shadowing is present.[9] Celebi *et al*. noted that lesions with posterior acoustic shadowing have at least one positive receptor.[10] In addition to confirming that posterior acoustic shadowing was associated with ER positive tumors, our study identified additional features. After adjusting for age and size, tumors with angulated or spiculated margins have >2.5 times the odds, and absence of hypoechoic features have lower (0.4 times) odds, for ER-positive tumors.

It has been reported that tumors with circumscribed margins occurred more often in triple-negative tumors.[10] We did not observe a statistical association between circumscribed margins and tripe-negative breast cancers. In a study of 344 invasive cancers of which 70 were triple-negative tumors, it was noted that they were more likely to present as hyperechoic tumors with an abrupt boundary and with posterior acoustic enhancement.[13] In this study, age-adjusted multivariable logistic regression model indicated that absence of posterior acoustic shadowing, and not necessarily the presence of posterior acoustic enhancement, was associated with triple-negative tumors. Our observations contradict Jung *et al*.,[13] in that we observed that tumors with hypoechoic features had more than twice the odds for being triple-negative tumors. We also did not observe an association between tumor boundary or margins and triple-negative tumors. We did observe that tumors with posterior acoustic shadow had lower odds (0.28 times) of being triple-negative tumors.

A prior study in which 33/181 (18.2%) patients with malignancies had germ line mutations in breast cancer genes BRCA1 and BRCA2, did not observe any noticeable US imaging characteristics that were specific to BRCA mutations.[14] Although our study observed a statistically positive correlation between posterior acoustic enhancement and BRCA1 mutation, this was non-specific and hence was not a significant predictor.

There were limitations. Although a large sample size, this was a single institutional retrospective study. Larger prospective trials from different centers and different geographic locations to corroborate these findings would be useful. During the study period, US elastography was not available at our institution. Hence, the association between parameters related to stiffness and tumor grade were not analyzed. The study focused on the US features of the index lesions and not the lymph nodes, as only a subset were node-positive due to the higher prevalence of T1 and T2 tumors in our cohort. The template for reporting at our institution included tumor size, shape, margins, echogenicity, and posterior features. Additional findings such as echogenic halo, peritumoral edema, necrosis, and skin involvement were not uniformly recorded and hence were not considered for analysis.

CONCLUSION

In our large series, US morphology, such as tumor size, margins, echogenicity, and posterior features showed significant association with tumor grade and receptor status. High-grade tumors were more hypoechoic, lacked angular or spiculated margins, and lacked posterior shadowing. ER/PR positive tumors were positively associated with irregular margins and posterior shadowing and negatively with tumor size and hypo-echogenicity. In our study, TNC had increasing tumor size, hypo-echogenicity, and lacked of posterior acoustic shadowing. The number of tumors with BRCA mutations was too small to make any meaningful conclusions. US morphology in our study was a good surrogate marker for tumor grade, receptor status and therefore helps corroborate histological findings where advanced laboratory facilities are available. In resource-limited settings where advanced laboratory support is lacking, US morphology could serve as a useful marker for the biological behavior of the tumor and guide treatment options.

Acknowledgments

This work was supported in part by the National Cancer Institute (NCI) of the National Institutes of Health (NIH)

grants R01 CA195512 and R01 CA199044. The contents are solely the responsibility of the authors and do not necessarily reflect the official views of the NCI or the NIH.

Declaration of patient consent

Institutional Review Board (IRB) permission obtained for the study.

Financial support and sponsorship

National Institutes of Health (NIH) grants R01 CA195512 and R01 CA199044 for this study.

Conflicts of interest

There are no conflicts of interest.

REFERENCES

1. Barr RG, DeVita R, Destounis S, Manzoni F, de Silvestri A, Tinelli C. Agreement between an automated volume breast scanner and handheld ultrasound for diagnostic breast examinations. J Ultrasound Med 2017;36:2087-92.
2. Vijayaraghavan GR, Vedantham S, Kataoka M, DeBenedectis C, Quinlan RM. The relevance of ultrasound imaging of suspicious axillary lymph nodes and fine-needle aspiration biopsy in the post-ACOSOG Z11 era in early breast cancer. Acad Radiol 2017;24:308-15.
3. Neuschler EI, Lavin PT, Tucker FL, Barke LD, Bertrand ML, Böhm-Vélez M, *et al*. Downgrading and upgrading gray-scale ultrasound BI-RADS categories of benign and malignant masses with optoacoustics: A pilot study. AJR Am J Roentgenol 2018;211:689-700.
4. Vijayaraghavan GR, Vedantham S, Santos-Nunez G, Hultman R. Unifocal invasive lobular carcinoma: Tumor size concordance between preoperative ultrasound imaging and postoperative pathology. Clin Breast Cancer 2018;18:e1367-72.
5. Raj SD, Phillips J, Mehta TS, Quintana LM, Fishman MD, Dialani V, *et al*. Management of BIRADS 3, 4A, and 4B lesions diagnosed as pure papilloma by ultrasound-guided core needle biopsy: Is surgical excision necessary? Acad Radiol 2019;26:909-14.
6. Dillon DA, Guidi AJ, Schnitt SJ. Pathology of invasive breast cancer. In: Harris JR, Lippman ME, Morrow M, Osborne CK, editors. Diseases of the Breast. 5th ed., Ch. 25. Philadelphia, PA: Lippincott-Williams & Wilkins; 2014.
7. Lamb PM, Perry NM, Vinnicombe SJ, Wells CA. Correlation between ultrasound characteristics, mammographic findings and histological grade in patients with invasive ductal carcinoma of the breast. Clin Radiol 2000;55:40-4.
8. Aho M, Irshad A, Ackerman SJ, Lewis M, Leddy R, Pope TL, *et al*. Correlation of sonographic features of invasive ductal mammary carcinoma with age, tumor grade, and hormone-receptor status. J Clin Ultrasound 2013;41:10-7.
9. Irshad A, Leddy R, Pisano E, Baker N, Lewis M, Ackerman S, *et al*. Assessing the role of ultrasound in predicting the biological behavior of breast cancer. AJR Am J Roentgenol 2013;200:284-90.
10. Celebi F, Pilanci KN, Ordu C, Ağacayak F, Alço G, İlgün S, *et al*. The role of ultrasonographic findings to predict molecular subtype, histologic grade, and hormone receptor status of breast cancer. Diagn Interv Radiol 2015;21:448-53.
11. Blaichman J, Marcus JC, Alsaadi T, El-Khoury M, Meterissian S, Mesurolle B. Sonographic appearance of invasive ductal carcinoma of the breast according to histologic grade. AJR Am J Roentgenol 2012;199:W402-8.
12. Adrada B, Wu Y, Yang W. Hyperechoic lesions of the breast: Radiologic-histopathologic correlation. AJR Am J Roentgenol 2013;200:W518-30.
13. Jung HK, Han K, Lee YJ, Moon HJ, Kim EK, Kim MJ. Mammographic and sonographic features of triple-negative invasive carcinoma of no special type. Ultrasound Med Biol 2015;41:375-83.
14. Mesurolle B, Kadoch L, El-Khoury M, Lisbona A, Dendukuri N, Foulkes WD. Sonographic features of breast carcinoma presenting as masses in BRCA gene mutation carriers. J Ultrasound Med 2007;26:817-24.
15. Firth D. Bias reduction of maximum-likelihood-estimates. Biometrika 1993;80:27-38.

How to cite this article: Vijayaraghavan GR, Kona M, Maheswaran A, Kandil DH, Toke MK, Vedantham S. Ultrasound imaging morphology is associated with biological behavior in invasive ductal carcinoma of the breast. J Clin Imaging Sci 2021;11:48.